was heated to 59.4° ± 0.1°C and the pressure was increased to 207 (± 0.5) bar by the addition of more CO_2 (a total of ~6.6 g of CO_2 added). The polymerization was continued at these conditions for 48 hours, during which time the system remained homogeneous and optically clear. At the end of the polymerization, CO_2 was vented and the polymer, which is not soluble in CO_2 at lower pressures, precipitated. The polymer and any unreacted monomer were quantitatively removed from the reaction vessel by dissolution in 1,1,2-trifluorotrichloroethane (Freon-113). The polymer was precipitated into a large excess of methanol, washed several times with methanol, and dried in vacuo overnight to give 3.25 g of transparent viscous polymer (yield: 65%). Fourier transform infrared (FTIR) (*14*) and ^1H nuclear magnetic resonance (NMR) (*15*) spectra showed that the polymer synthesized in CO_2 was identical to the polymer made in CFCs. Gel permeation chromatography (GPC) indicated that the polymer made in CO_2 had a molar weight of ~270,000 g/mol (*16*). Similar results could be obtained for a variety of other highly fluorinated acrylic monomers whose corresponding homopolymers are essentially insoluble in all traditional solvents except CFCs.

Polymer synthesis in supercritical CO_2 was also extended to statistical copolymers of fluorinated monomers with conventional hydrocarbon-based monomers such as methyl methacrylate, butyl acrylate, styrene, and ethylene. The corresponding homopolymers of the conventional hydrocarbon monomers are essentially insoluble in CO_2 at these conditions (*3*). Copolymers of FOA were made under similar conditions as described above. The molar ratios of the monomers in the feed, f_1, and the molar ratios incorporated into the copolymer, F_1, are given in Table 1. Homogeneous copolymerizations could be maintained even with very high concentrations of comonomer as shown.

Supercritical CO_2 is an excellent alternative to CFCs for conducting homogeneous solution homo- and copolymerization of fluorinated monomers. Under the conditions used here, we found that AIBN decomposes at a rate 2.5 times slower in CO_2 than in benzene but with greater efficiency. We have demonstrated that it is possible to synthesize high molar mass homo- and copolymers of fluorinated monomers in a homogeneous fashion in supercritical CO_2. This new process for the synthesis of fluoropolymers and copolymers points to the potential for using supercritical CO_2 in other solution polymerizations such as group transfer polymerization, living cationic polymerizations, and perhaps even some anionic polymerizations whose active chain end could be stabilized in CO_2.

REFERENCES AND NOTES

1. S. Solomon, R. R. Garcia, F. Sherwood, D. J. Wuebbles, *Nature* **321**, 755 (1986).
2. L. Wall, Ed., *Fluoropolymers, High Polymers* (Wiley-Interscience, New York, 1972), vol. 25.
3. M. McHugh and V. J. Krukonis, *Supercritical Fluid Extraction—Principles and Practice* (Butterworths, Boston, 1986), chap. 9.
4. B. Subramaniam and M. A. McHugh, *Ind. Eng. Chem. Process Des. Dev.* **25**, 1 (1986); W. M. Flarsheim, Y. Tsou, I. Trachtenberg, K. P. Johnston, A. J. Bard, *J. Phys. Chem.* **90**, 3857 (1986); S. Kim and K. P. Johnston, *Ind. Eng. Chem. Res.* **26**, 1206 (1987); K. P. Johnston and C. Haynes, *AIChE J.* **33**, 2017 (1987); S. Kim and K. P. Johnston, *Chem. Eng. Commun.* **63**, 49 (1987); G. C. Alexander and M. E. Paulaitis, *Pure Appl. Chem.* **59**, 61 (1987); T. Aida and T. G. Squires, *ACS Symp. Ser.* **329**, 58 (1987); R. M. Crooks and A. J. Bard, *J. Phys. Chem.* **91**, 1274 (1987); C. R. Cabrera and A. J. Bard, *J. Electroanal. Chem.* **273**, 147 (1989); D. C. Peck, A. J. Mehta, K. P. Johnston, *J. Phys. Chem.* **93**, 4297 (1989); B. J. Hrnjez, A. J. Mehta, M. A. Fox, K. P. Johnston, *J. Am. Chem. Soc.* **111**, 2662 (1989); K. P. Johnston, G. J. McFann, D. Peck, R. M. Lemert, *Fluid Phase Equilib.* **52**, 337 (1989); S. M. Howdle, M. A. Healy, M. Poliakoff, *J. Am. Chem. Soc.* **112**, 4804 (1990); M. Jobling, S. M. Howdle, M. Poliakoff, *J. Chem. Soc. Chem. Commun.* **1990**, 1762 (1990); B. C. Wu, M. T. Klein, S. I. Sandler, *Ind. Eng. Chem. Res.* **30**, 822 (1991).
5. J. M. DeSimone and Z. Guan, unpublished material.
6. G. Odian, *Principles of Polymerization* (Wiley, New York, 1981), chap. 3.
7. J. P. Van Hook and A. V. Tobolsky, *J. Am. Chem. Soc.* **80**, 779 (1958).
8. R. M. Lemert and J. M. DeSimone, *J. Supercrit. Fluids* **4**, 186 (1991).
9. G. S. Hammond, O. D. Trapp, R. T. Keys, D. L. Neff, *J. Am. Chem. Soc.* **81**, 4878 (1959); G. S. Hammond, C. S. Wu, O. D. Trapp, J. Warkentin, R. T. Keys, *ibid.* **82**, 5394 (1960).
10. The significant decrease in the rate of AIBN decomposition in supercritical CO_2 is primarily the result of solvation effects as there is a negligible static pressure effect on its decomposition rate in liquid solvents; see A. H. Ewald, *Discuss. Faraday Soc.* **22**, 138 (1956).
11. Others have shown a systematic dependence on dielectric strength for the decomposition of AIBN in liquid solvents; see O. Yamamoto, J. Yamashita, H. Hashimoto, *Kogyo Kagaku Zasshi* **71**, 223 (1968).
12. P. D. Bartlett and T. Funahashi, *J. Am. Chem. Soc.* **84**, 2596 (1962).
13. K. E. O'Shea, J. R. Combes, M. A. Fox, K. P. Johnston, *Photochem. Photobiol.* **54**, 571 (1991).
14. FTIR: 1758 cm^{-1} (strong carbonyl absorption); 1120 to 1350 cm^{-1} (strong C–F absorption).
15. ^1H NMR (1,1,2-trifluorotrichloroethane with $CDCl_3$ in sealed capillary in annulus, 200 MHz, 23°C): δ 2.12 and 1.81 (m, 2H); δ 2.47 (s, 1H); δ 4.59 (t, 2H).
16. Molar masses were measured with GPC with a 1,1,2-trifluorotrichloroethane mobile phase and fluoropolymer molecular weight standards.

17. We gratefully acknowledge financial support from the University of North Carolina at Chapel Hill, E. I. duPont de Nemours & Co., Inc., 3M Company, and Unilever Research.

28 April 1992; accepted 25 June 1992

Internal Stark Effect Measurement of the Electric Field at the Amino Terminus of an α Helix

David J. Lockhart and Peter S. Kim

The strengths of electrostatic interactions in biological molecules are difficult to calculate or predict because they occur in complicated, inhomogeneous environments. The electric field at the amino terminus of an α helix in water has been determined by measuring the shift in the absorption band for a covalently attached, neutral probe molecule with an electric dipole moment difference between the ground and excited electronic states (an internal Stark effect). The field at the interface between the helix and the solvent is found to be an order of magnitude stronger than expected from the dielectric properties of bulk water. Furthermore, although the total electric dipole moment of the helix increases with length, the electric field at the amino terminus does not.

Interactions involving charged and polar groups are important determinants of the properties of biological macromolecules. Theoretical assessment of these electrostatic interactions is difficult because they occur in complicated environments and frequently near solvated surfaces of irregular shape and composition. Determining the strength of electrostatic interactions is a difficult experimental problem as well. The standard methods involve: (i) measuring the change in the pK_a (K_a, acid dissociation constant) of an ionizable group; or (ii) mutating a charged or polar group and measuring the change in stability or function. Although these measurements depend on the electrostatic potential at a particular position in the folded state, the physical interpretation of the results is complicated by structural relaxation, differences in solvation of the mutated or charged groups, and changes in the unfolded state.

We have developed a method to measure the electric field (instead of the potential) that uses a relatively nonperturbing, uncharged probe molecule. The method is used to measure the electric field at the amino termini of short, stable, monomeric α helices in water. The results are straightforward to interpret because the field does not have to be inferred from the effects of

Howard Hughes Medical Institute, Whitehead Institute for Biomedical Research, Department of Biology, Massachusetts Institute of Technology, Nine Cambridge Center, Cambridge, MA 02142.

changes in side chain charge or identity. To our knowledge, there is no other way to measure directly and quantitatively the electric field in this type of environment.

The peptide bond has a dipolar charge distribution, and in an α helix the individual peptide dipoles are nearly aligned with the helix axis. This arrangement results in a large electric dipole moment, estimated to be ~3.5 D per residue (*1*, *2*). The dipolar charge distribution of helices is expected to produce an electric field that may influence, for example, protein folding, protein stability, ligand binding, and enzymatic reactions (*2*–*4*).

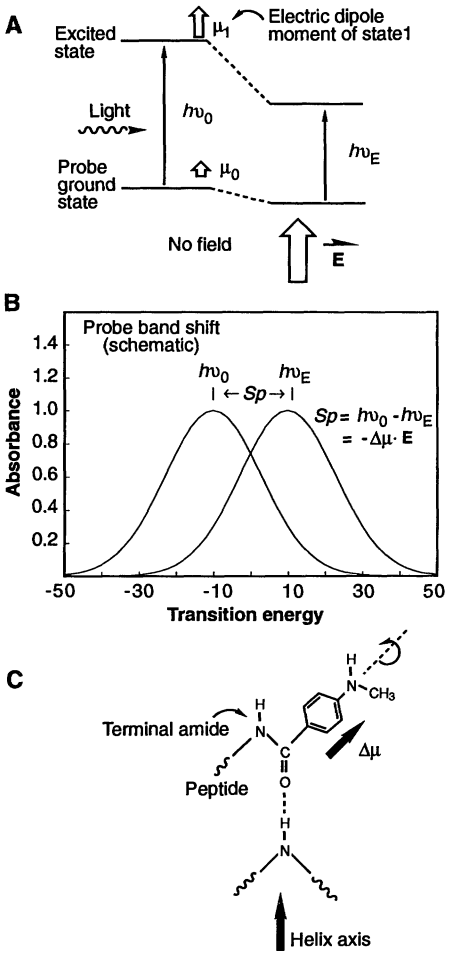

Fig. 1. Physical basis of the internal Stark effect. (**A**) The effect of an electric field **E** on the energy difference between two states and (**B**) the resulting change in the absorption spectrum. The transition energy changes if μ_1 (the permanent electric dipole moment of state 1) is not equal to μ_0, leading to a band shift (denoted *Sp*) of $-\Delta\mu\cdot\mathbf{E}$, where $\Delta\mu = \mu_1 - \mu_0$. (**C**) Schematic of the probe molecule attached covalently to the amino terminus of a peptide, including the hydrogen bond between the probe carbonyl oxygen and the amide NH of residue 4. Rotation of the probe about the axis drawn does not affect the direction of $\Delta\mu$. In the figure, h is Planck's constant, and ν_0 and ν_E denote the frequency of light for the optical transition in the absence and presence of the electric field **E**.

The method (Fig. 1) involves the covalent attachment of a neutral aromatic probe molecule to a peptide. In the presence of an electric field (the electric field is the force per unit charge and is proportional to the derivative of the electrostatic potential), the energies of the various electronic states of the probe change (to first order) by an amount $-\mu_i\cdot\mathbf{E}$, where **E** is the electric field at the probe and μ_i is the permanent electric dipole moment of the i^{th} electronic state (Fig. 1A). In the presence of **E**, the energy difference between two states i and j changes by $-\Delta\mu\cdot\mathbf{E}$, where $\Delta\mu = \mu_j - \mu_i$. If state i is the ground electronic state and state j is an excited electronic state that can be reached by the absorption of light, an electric field at the probe changes the transition energy by $-\Delta\mu\cdot\mathbf{E}$. If $\Delta\mu$ is known, the electric field can be determined simply by a measurement of the shift in the corresponding absorption band (Fig. 1B).

The primary probe molecule used in these experiments is 4-(methylamino)benzoic acid (MABA), which is attached to the amino terminus of the peptides through an amide linkage (Fig. 1C). The carbonyl of the amide link acts as a helical hydrogen-bond acceptor for the backbone amide proton of residue 4. In this arrangement, confirmed by nuclear magnetic resonance (NMR) studies presented below, the position of the probe is well defined except for a ring flip that does not affect the direction of $\Delta\mu$ (Fig. 1C).

Neutral MABA attached to a peptide has an absorption band centered near 295 nm with a maximum extinction coefficient of ~19,000 M^{-1} cm^{-1} (*5*). The electric dipole moment difference, $\Delta\mu$, for this transition is measured with Stark effect (or electromodulation) spectroscopy (*6*) to be 8 D (*7*). We take $\Delta\mu$ to be in the direction shown in Fig. 1C, as is found for several para-substituted benzene derivatives (*8*).

The peptides used in these experiments are the following (*9*):

F_S: -AAAAA(AAARA)$_3$A-CONH$_2$
F_L: -AAAAA(AAARA)$_7$A-CONH$_2$
U_S: -AAPAA(APARA)$_3$A-CONH$_2$

F_SR5: -(AAAAR)$_4$A-CONH$_2$
U_SR5: -(AAPAR)$_4$A-CONH$_2$

F_LR5: -(AAAAR)$_8$A-CONH$_2$
U_LR5: -(AAPAR)$_8$A-CONH$_2$

where A is Ala, R is Arg, and P is Pro; F and U indicate peptides designed to be folded or unfolded, respectively; the subscripts S and L denote short peptides and their longer versions and R5 denotes the presence of an Arg residue at position 5.

Sixteen residue peptides based on the repeating unit (A-A-A-A-K), where K is Lys, have been found to be monomeric and up to 80% helical in water (*10*). Longer peptides are used here to increase helical content and stability. We use Arg instead of Lys because it has a slightly greater helical propensity (*11*). The peptide F_S contains only Ala at positions 1 through 8 in order to minimize the effects of side chain charges on the properties of the amino-terminal probes. We do not include Tyr and Trp because absorption bands near 280 nm overlap with those of the probes and would interfere with the band-shift measurements.

The U_S and U_L peptides serve as unfolded controls. These peptides have Ala at positions 1 and 2 near the probe, but contain several prolines to disrupt structure. The unfolded control molecules allow

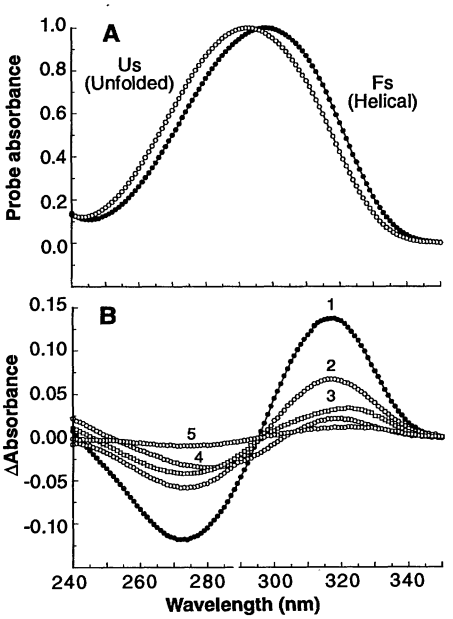

Fig. 2. In the presence of helical structure, the probe absorption band shifts by ~5 nm, corresponding to a change in the transition energy of 550 cm^{-1} or 1.6 kcal/mol. This band shift is diminished by factors that disrupt structure, and also at high ionic strength. (**A**) Absorption spectrum of MABA attached to F_S (closed circles) and U_S (open circles) (0°C, pH 7) (*23*). (**B**) Absorption difference spectra (F_S minus U_S) under different conditions. The amplitudes of the peaks in the difference spectra are approximately proportional to the band shift. Curve 1 is the difference at 0°C, 0 M NaCl and 0 M guanidinium hydrochloride (GuHCl). For curves 2 to 4, one condition was changed: curve 2, 80°C; curve 3, 4 M NaCl; and curve 4, 6 M GuHCl. Curve 5 is the difference at 0°C, 0 M NaCl, and 0 M GuHCl for peptides identical to F_SR5 and U_SR5 but with Gly-Gly added at the amino terminus between the probe and the peptide.

the properties of the attached probes to be measured in the absence of helical structure but otherwise identical conditions.

Circular dichroism (CD) experiments show that the peptides designed to be structured are highly helical (≥90% at 0°C) and that the control peptides are unstructured (*12*). Two-dimensional (2D) NMR experiments indicate that the helix extends to the amino terminus in peptide F_S (see below). The helical peptides are monomeric (*13*), water soluble (>3 mM), and quite stable (with MABA attached, the 21-residue peptides F_S and F_SR5 have melting temperatures of 35° and 32°C, respectively, and the 41-residue peptides F_L and F_LR5 melt at 50°C).

In the presence of helical structure, the absorption band of the MABA probe is shifted by ~5 nm (Fig. 2A). This band shift corresponds to a change in the transition energy of 550 cm^{-1} or 1.6 kcal/mol. The probe band shift is similar when attached to F_S, F_L, F_SR5, and F_LR5 (relative values of 1.0, 1.0, 0.96, and 0.92 ± 0.05, respectively), indicating that the observed field at the amino terminus is produced primarily by the helical backbone dipoles (that is, not side chain charges) and is independent of helix length between 21 and 41 residues.

The probe band shift is diminished significantly when the peptide structure is disturbed and also at high ionic strength. The shift is reduced (Fig. 2B) by: (i) an increase in temperature; (ii) the chemical denaturant guanidinium hydrochloride (GuHCl); (iii) the addition of a Gly-Gly spacer between the amino terminus of the helix and the probe; and (iv) the addition of 4 M NaCl (*14*).

In order to verify that the observed effect depends on $\Delta\mu$ and not, for example, on changes in hydrogen bonding or other specific interactions, the band shift is measured with three other probes attached to the peptides. The other probe groups are 4-aminobenzoic acid (ABA), terephthalic acid (1,4-dibenzoic acid, TPA), and 4-nitrobenzoic acid (NBA). ABA has electronic properties similar to MABA, TPA has a smaller $\Delta\mu$ because it is more symmetric than either MABA or ABA, and in NBA, the direction of $\Delta\mu$ is opposite that for MABA and ABA [see (*8*)]. The band shift for ABA is nearly identical to that for MABA. The shift measured for TPA is smaller by more than a factor of 3, and the shift for NBA is in the opposite direction (*15*). These results provide strong evidence that the probes are responding to the electric field at the amino terminus, as shown in Fig. 1.

The alignment of dipolar peptide bonds in an α helix results in a significant electric dipole moment for the entire helix (*1*, *2*), often referred to as the helix macrodipole. This property has been invoked to explain stability changes in peptides and proteins when charges are placed near helix termini (*2–4*, *16*). The most appropriate simple model of the helix dipole is that of a line dipole with the dipole density (mostly from the peptide bonds) distributed along the length of the helix (*1*, *2*). Although the total dipole moment of the helix increases with length, the addition of helical residues at the carboxyl terminus is expected to have little effect on interactions that occur near the amino terminus because the strength of electrostatic interactions decreases rapidly with distance (the magnitude of the dipolar

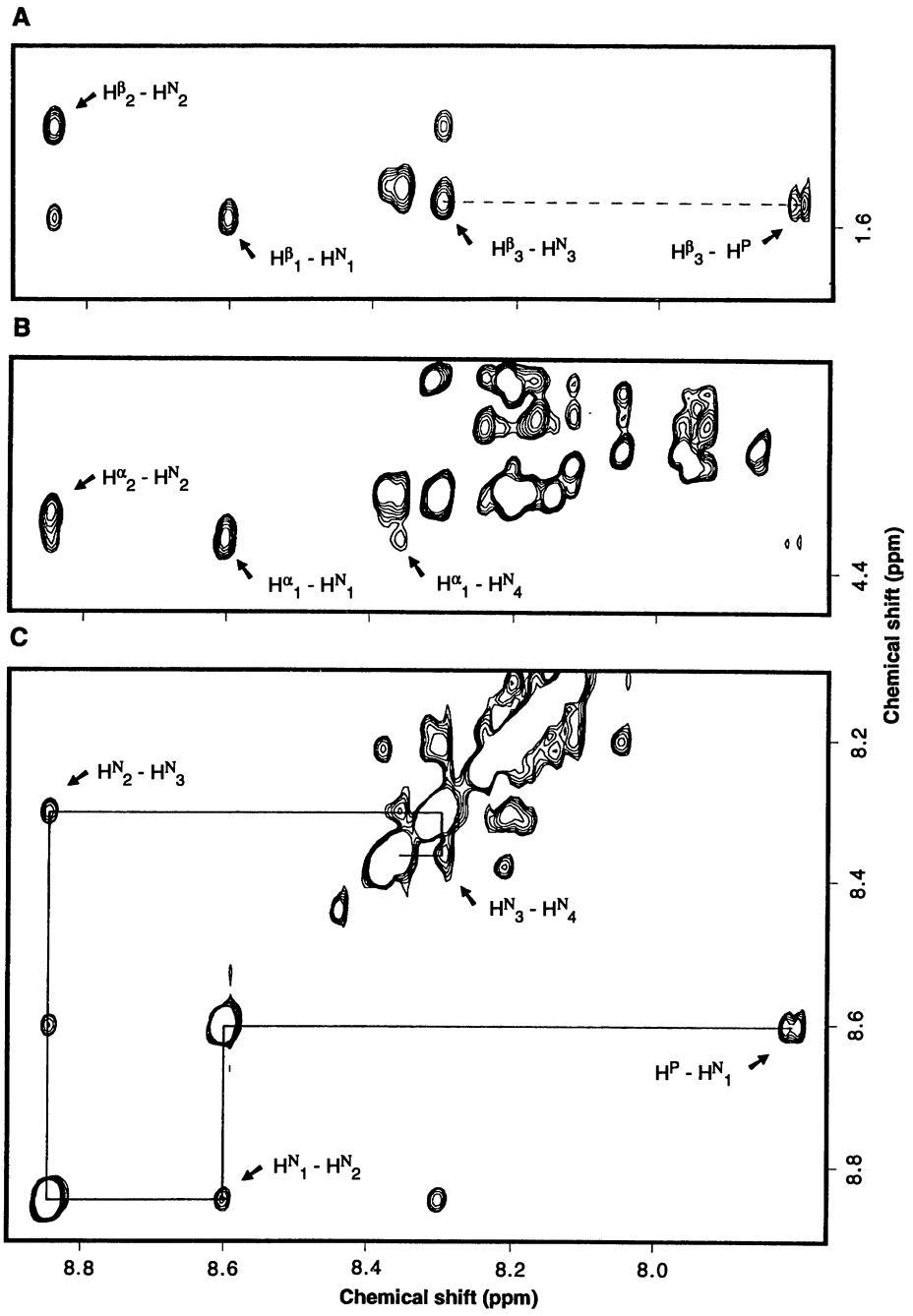

Fig. 3. Data from 2D-NMR experiments indicate that the amino terminus of the peptide is helical and that the probe is in a well-defined position. The NOESY data obtained on the selectively deuterated version of the 21-residue helical peptide F_S with MABA attached are shown (*24*). (**A**) The amide and aromatic $-H^{\beta}$ region, (**B**) the $H^N - H^{\alpha}$ region, and (**C**) the H^N and aromatic region of the NOESY spectrum. In (C), the NOE connectivities are shown starting from the probe aromatic proton resonances (H^P) and then proceeding sequentially to the amide protons of the first four residues. The contour level is the same in (A) and (C) and a lower level is shown in (B). The identities of the $H^N_i - H^{\alpha}_i$ crosspeaks in (B) were confirmed by 2D correlation spectroscopy (COSY) experiments under identical conditions.

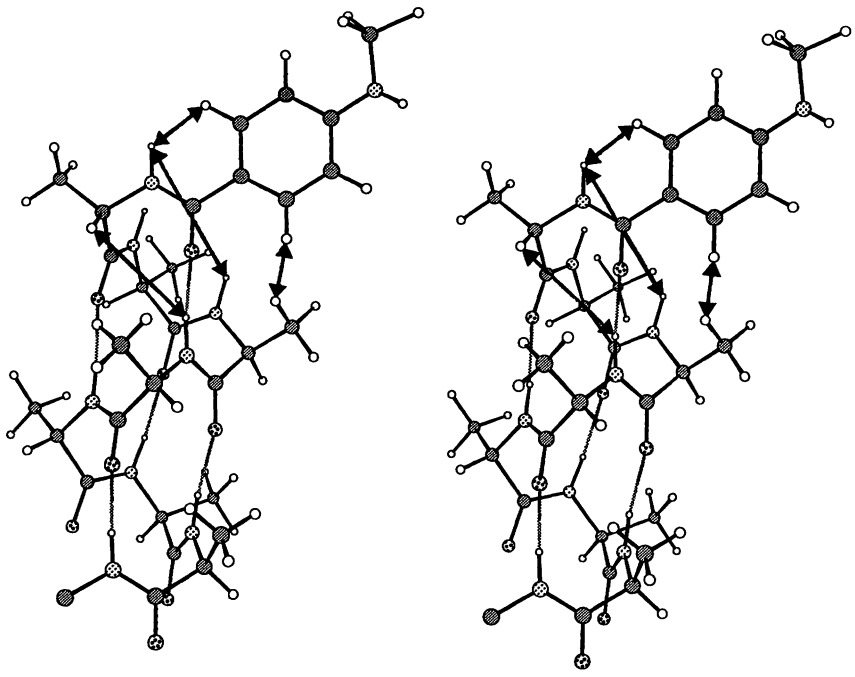

Fig. 4. Stereo illustration of the probe (MABA) at the amino terminus of two turns of an α helix. The arrows connect protons that give rise to observable NOE crosspeaks. Only a few of the most important NOEs are indicated: $H^P - H^{N}_1$, $H^{\beta}_3 - H^P$, $H^{\alpha}_1 - H^{N}_4$, and $H^{N}_1 - H^{N}_3$.

Table 1. Nonsequential amino-terminal nuclear Overhauser effect crosspeaks (NOEs). The proton-proton distances are calculated with the backbone fixed as shown in Fig. 4 and with the MABA ring in the plane of the amide bond between the backbone and the probe. For NOEs involving β protons, the range of minimum distances between equivalent protons is given.

Observed NOE	Relative intensity	Expected distance (Å)
H^{N}_1-H^{N}_3	Weak	4.3
H^{N}_2-H^{N}_4	Weak	4.3
H^{N}_1-H^{N}_4	Weak	4.7
H^{α}_1-H^{N}_4	Moderate	3.4
H^{α}_1-H^{β}_4	Moderate	2.5–3.0
H^{β}_3-H^P	Strong	1.8–2.4
H^P-H^{N}_1	Strong	1.8
H^P-H^{N}_2	Weak	3.9
H^P-H^{N}_3	Weak	3.5
$H^P H^{N}_4$	Weak	3.4

electric field is inversely proportional to the distance cubed). These expectations are supported by recent theoretical calculations (*4*). Our results provide an experimental demonstration that the electric field at the amino terminus is essentially independent of helix length between 21 and 41 residues.

From the CD measurements, it is clear that the peptides are highly helical. For the band-shift results to be interpreted quantitatively, however, it is necessary to determine that the amino terminus is structured (that is, not frayed) and that the probe is in a well-defined position relative to the helix backbone. More detailed verification of amino-terminal structure is provided by 2D-NMR experiments on a selectively deuterated version of the peptide F_S with MABA attached. In this peptide, all of the Ala β protons are replaced with deuterons except those of Ala residues 1 to 4. The NMR data are shown in Fig. 3 and a structural model is shown in Fig. 4.

The amide proton resonance of Ala^1 (H^{N}_1) is assigned by the large nuclear Overhauser effect (NOE) crosspeak to the nearby probe aromatic protons (denoted H^P). Sequential amide-amide NOEs can then be followed to the amide proton resonance of Ala^4 (Fig. 3C). Weaker nonsequential amide NOE crosspeaks are also observed (Table 1). These data indicate that the amino terminus of the peptide is highly structured and not frayed to a significant extent (*17*).

The NOE crosspeaks observed between the H^P resonance and resonances of protons in the first turn of the helix (see Table 1) indicate that the probe is in a well-defined position. Most important is the strong crosspeak between H^P and the β proton resonance of Ala^3 (Fig. 3A) which indicates that the probe is positioned significantly closer to the methyl group of Ala^3 than to the other methyl groups, as shown in Fig. 4. The crosspeaks used to establish the structure of the amino terminus are not observed in nuclear Overhauser and exchange spectroscopy (NOESY) experiments performed on the unfolded control peptide U_S with MABA attached (*18*).

The net effect of the environment on the field can be determined by comparing the magnitude of the electric field measured experimentally with the value calculated with Coulomb's law and a dielectric constant of 1 (that is, as if there is no environment). The magnitude of the experimentally observed shift, denoted *Sp*, is related to the electric field **E** by the expression

$$Sp = |\Delta\mu|\,|\mathbf{E}|\cos\theta$$

where θ is the angle between Δμ and **E**. Given the measured values for *Sp* and $|\Delta\mu|$ (1.6 kcal/mol and 8 D, respectively), $|\mathbf{E}|\cos\theta$ is equal to 4.1×10^6 V/cm. The calculated electric field, $\mathbf{E}_c$, is 3.4×10^7 V/cm, and the calculated angle, θ_c, between the field and Δμ is ~20° (*19*). The effective dielectric constant ε_{eff} is defined as the ratio of the field calculated from simple vacuum electrostatics and the experimentally observed value:

$$\varepsilon_{eff} = (|\mathbf{E}_c|\cos\theta_c)/(|\mathbf{E}|\cos\theta)$$
$$= (3.4 \times 10^7)(\cos 20°)/(4.1 \times 10^6) \approx 8$$

Although diminished by the environment, the field measured at the boundary between the peptide and water is still an order of magnitude stronger than expected based on the dielectric properties of bulk water (the dielectric constant of water is 88 at 0°C). An ε_{eff} between 2 and 4 is usually used for the interiors of proteins (*4*, *20*, *21*). In contrast, a larger effective dielectric constant (between 30 and 100) is considered appropriate for interactions involving unpaired charges, especially if the charges are solvent-accessible (*20*, *22*) (a large value is consistent with our observation that a charged Arg side chain at position 5 in peptide F_SR5 does not affect the band shift significantly). The value of eight determined here should be appropriate for estimating the strength of short-range dipole-dipole interactions that occur near protein surfaces, such as those involved in ligand binding and enzymatic reactions.

REFERENCES AND NOTES

1. A. Wada, *Adv. Biophys.* **9**, 1 (1976).
2. W. G. J. Hol, P. T. van Duijnen, H. J. C. Berendsen, *Nature* **273**, 443 (1978).
3. W. G. J. Hol, L. M. Halie, C. Sander, *ibid.* **294**, 532 (1981).
4. J. Aqvist, H. Luecke, F. A. Quiocho, A. Warshel, *Proc. Natl. Acad. Sci. U.S.A.* **88**, 2026 (1991).
5. The extinction coefficient for MABA attached to a peptide is determined from quantitative amino acid analysis (Arg content) of solutions of known absorbance.
6. W. Liptay, in *Excited States*, E. C. Lim, Ed. (Academic Press, New York, 1974), vol. 1, pp. 129–229; R. Mathies and L. Stryer, *Proc. Natl. Acad. Sci. U.S.A.* **73**, 2169 (1976); D. J. Lockhart and S. G. Boxer, *Biochemistry* **26**, 664 (1987).
7. D. J. Lockhart, D. W. Pierce, S. G. Boxer, unpublished results.

8. S. K. Hemant and K. Yates, *J. Am. Chem. Soc.* **113**, 6062 (1991).
9. The peptides, except the specifically deuterated one (see Fig. 3), were synthesized on an Applied Biosystems Model 431A peptide synthesizer with Fmoc/HBTU [9-fluorenyl methoxy carbonyl/2-(1*H*-benzotriazol-1-yl)-1,1,3,3-tetramethyluronium hexafluorophosphate] cycles [C. G. Fields, D. H. Lloyd, R. L. Macdonald, K. M. Otteson, R. L. Noble, *Peptide Res.* **4**, 95 (1991)] modified to include acetic anhydride capping. The probes are coupled to the peptides by using HBTU activation and ~30-fold molar excess of activated species to peptide-resin. Each reaction is allowed to proceed for 2 to 3 hours. The peptides (with probes attached) are cleaved from the resins by using standard Fmoc protocols, with final purification by reversed-phase high-performance liquid chromatography. The identity of the peptides with probes attached is confirmed by mass spectrometry (Mass-Search, Inc., Modesto, CA).
10. S. Marqusee, V. H. Robbins, R. L. Baldwin, *Proc. Natl. Acad. Sci. U.S.A.* **86**, 5286 (1989).
11. K. T. O'Neil and W. F. DeGrado, *Science* **250**, 646 (1990); G. Merutka and E. Stellwagen, *Biochemistry* **30**, 1591 (1991).
12. The F peptides with MABA attached have CD spectra (0°C, pH 7) typical of α helices [R. W. Woody, in *The Peptides*, S. Undenfriend, J. Meienhofer, J. R. Hruby, Eds. (Academic Press, New York, 1985), vol. 7, pp. 15–114], with minima at 222 and 208 nm. With MABA attached, $[\theta]_{222}$ for F_S and F_SR5 is −32,100 and −32,300 degree cm²/dmol, respectively, and −39,900 and −40,600 for the longer F_L and F_LR5 peptides. $[\theta]_{208}$ for F_S, F_SR5, F_L, and F_LR5 is −25,600, −26,500, −31,400, and −32,300 degree cm²/dmol, respectively. These CD data and measurements of GuHCl-induced unfolding of F_S with MABA attached (D. J. Lockhart and P. S. Kim, unpublished results) suggest that the 21-residue peptides are greater than 90% helical and that the 41-residue peptides are nearly 100% helical. The CD spectra of the U peptides with MABA indicate that they are unstructured. At 0°C, the CD spectrum of peptide U_S with MABA attached has a maximum of +510 degree cm²/dmol at 227 nm and a value at 222 nm of approximately +100 degree cm²/dmol. The CD data are obtained in a 1-cm cell with an Aviv Associates 62DS Circular Dichroism spectrometer.
13. The melting temperatures for the helical peptides, determined by the temperature dependence of the CD signal at 222 nm, are independent of peptide concentration (measured between 4 and 70 μM, and up to 4 mM for peptide F_S). The unfolded peptides have concentration-independent CD spectra at 0°C between 4 and 70 μM.
14. The probe band shift decreases by ~20% of the maximum value per molar increase in monovalent salt concentration (similar effects have been observed with NaCl, LiCl, and KF), even though salt does not affect peptide structure (<3% variation in the CD signal at 222 nm between 0 and 3 M NaCl at 0°C). The dependence of the field on ionic strength is weak probably because the helix backbone dipoles are not completely accessible to ions or solvent molecules and the dipolar field decreases rapidly with distance.
15. The observed shifts (relative to a value of 1.0 for MABA attached to F_S at 0°C) for the other probes attached to peptide F_S at 0°C are: 0.95 ± 0.05 for ABA; ≤0.3 for TPA; and −0.12 ± 0.05 for NBA.
16. K. R. Shoemaker, P. S. Kim, E. J. York, J. M. Stewart, R. L. Baldwin, *Nature* **326**, 563 (1987); D. Sali, M. Bycroft, A. R. Fersht, *ibid.* **335**, 740 (1988); H. Nicholson, W. J. Becktel, B. W. Matthews, *ibid.* **336**, 651 (1988); R. Fairman, K. R. Shoemaker, E. J. York, J. M. Stewart, R. L. Baldwin, *Proteins* **5**, 1 (1989); L. Serrano and A. R. Fersht, *Nature* **342**, 296 (1989); H. Nicholson, D. E. Anderson, S. Dao-pin, B. W. Matthews, *Biochemistry* **30**, 9816 (1991); J. Sancho, L. Serrano, A. R. Fersht, *ibid.* **31**, 2253 (1992).
17. A small degree of fraying, however, cannot be ruled out, and the probe band shift is expected to be approximately proportional to the percentage of time that the amino-terminal residues are in a helical conformation. If the amino terminus near the probe is slightly frayed [A. Chakrabartty, J. A. Schellman, R. L. Baldwin, *Nature* **351**, 586 (1991); M. I. Liff, P. C. Lyu, N. R. Kallenbach, *J. Am. Chem. Soc.* **113**, 1014 (1991); S. M. Miick, A. P. Todd, G. L. Millhauser, *Biochemistry* **30**, 9498 (1991); C. A. Rohl, J. M. Scholtz, E. J. York, J. M. Stewart, R. L. Baldwin, *ibid.* **31**, 1263 (1992)], then the electric field measured here represents a lower limit, and ε_{eff} is smaller than the value we have calculated.
18. D. J. Lockhart and P. S. Kim, unpublished results. The only exception is the $H^P - H^N{}_1$ crosspeak, which is expected even in the unfolded peptides.
19. A 21-residue Ala α helix is built with partial charges assigned by the CHARMM [B. R. Brooks *et al.*, *J. Comput. Chem.* **4**, 187 (1983)] parameter set (PARAM19) and the electric field at the center of the probe is calculated by using a dielectric constant of 1. The calculated field for a 41-residue helix is larger by less than 1%.
20. M. K. Gilson, A. Rashin, R. Fine, B. Honig, *J. Mol. Biol.* **183**, 503 (1985); M. K. Gilson and B. H. Honig, *Biopolymers* **25**, 2097 (1986); M. K. Gilson and B. Honig, *Proteins* **3**, 32 (1988); D. Bashford and M. Karplus, *Biochemistry* **29**, 10219 (1990).
21. K. K. Rodgers and S. G. Sligar, *J. Am. Chem. Soc.* **113**, 9419 (1991).
22. D. C. Rees, *J. Mol. Biol.* **141**, 323 (1980); A. J. Russel and A. R. Fersht, *Nature* **328**, 496 (1987); D. Sali, M. Bycroft, A. R. Fersht, *J. Mol. Biol.* **220**, 779 (1991).
23. The sample concentration for the optical experiments is typically 15 μM. The buffer for all optical experiments contains 1 mM sodium citrate, 1 mM sodium phosphate, and 1 mM sodium borate with no added salt unless specified. The absorption data are recorded in a 1-cm pathlength cell at 0°C and pH 7, unless specified otherwise, with an Aviv Associates 14DS or 118DS spectrophotometer.
24. Two-dimensional NMR data were collected on ~4 mM samples in 100 mM sodium phosphate (pH 4.5) at 3°C. Data were collected on a Bruker AMX 500 MHz spectrometer. NOESY experiments are performed with a mixing time of 200 ms. Chemical shift is relative to TMSP [2,2,3,3-tetradeutero-3-(trimethylsilyl)-propionic acid sodium salt]. The specifically deuterated peptide is synthesized on an Applied Biosystems Model 430A peptide synthesizer using standard t-Boc/NMP (*tert*-butyloxycarbonyl/*N*-methylpyrrolidone) cycles modified to include acetic anhydride capping. t-Boc-L-alanine[3,3,3-D3] is obtained from Tracer Technologies (Somerville, MA). The peptide is cleaved with a standard t-Boc cleavage procedure (low-high trifluoromethanesulfonic acid).

25. We thank R. Rutkowski, M. Milhollen, and M. Burgess for peptide synthesis and attachment of the probes; P. Hoeprich for discussions concerning synthesis; S. Stradley for amino acid analysis; Z.-y. Peng, B. Schulman, L. McIntosh, K. Lumb, and C. J. McKnight for help with NMR; B. Tidor for help with CHARMM; B. Tidor, S. Boxer and the Kim group for discussion and critical reading of the manuscript; and D. Pierce, D. Oh, and M. Steffen for help with Stark effect measurements. D.J.L. is supported by a Damon Runyon–Walter Winchell Cancer Research Fund Fellowship. P.S.K. is a Pew Scholar in the Biomedical Sciences and a Rita Allen Foundation Scholar. This research was supported by the Howard Hughes Medical Institute.

8 May 1992; accepted 9 July 1992

The Reversal and Splitting of Waves in an Excitable Medium Caused by an Electrical Field

Hana Ševčíková, Miloš Marek, Stefan C. Müller

The reversal and splitting of traveling concentration waves was observed in a one-dimensional Belousov-Zhabotinski reaction medium under the influence of low-intensity electric field gradients (~10 V per centimeter). The wave reversal and splitting were strongly correlated with a characteristic transformation of the shape of both the wave front and the refractory tail of a wave in the local field gradient. The secondary role of generated hydrodynamic flow on wave transformation was also investigated.

Traveling waves are highly organized spatio-temporal patterns of system variables (component concentration and electrical potential) that very often underlie transmission of information, growth, and developmental processes in cells and living tissues (*1–4*) and other types of excitable systems (*5*). These wave patterns are produced because of the interaction of transport processes with the processes of ionic species production and consumption. These waves often have a relaxational character where the short excited front of a wave with a high amplitude of system variables is followed by a long refractory region with a very low amplitude. Because of this refractory region, the excitable waves cannot be reflected at the impermeable barriers, refract, or pass through each other, unlike sound or light waves. Despite this, several examples have been reported that show that under certain circumstances, the refractoriness of an excitable system can be suppressed and the phenomena similar to refraction or soliton-like behavior (*6–8*) can occur. This report describes in a semiquantitative way the mechanism of system changes that occur in the course of the reversal and splitting of a wave traveling in a capillary tube filled with a mixture that supports the Belousov-Zhabotinski (BZ) reaction and is exposed to the external electric field.

H. Ševčíková and M. Marek, Department of Chemical Engineering, Prague Institute of Chemical Technology, Technicka 5, 166 28 Prague 6, Czechoslovakia. S. C. Müller, Max-Planck-Institut für Ernährungsphysiologie, Rheinlanddamm 201, W-4600 Dortmund 1, Germany.